J|A|C|S
ARTICLES
Published on Web 04/06/2007

Tetraazachlorin−Fullerene Conjugates: On−Off Control of Electronic Communication Enabled by Push−Pull Substituents

Takamitsu Fukuda, Satoshi Masuda, and Nagao Kobayashi*

Contribution from the Department of Chemistry, Graduate School of Science, Tohoku University, Sendai 980-8578, Japan

Received November 2, 2006; E-mail: nagaok@mail.tains.tohoku.ac.jp

Abstract: Novel tetraazachlorin (TAC)−fullerene (C_{60}) conjugates (TAC−C_{60}) and their analogues (TAiBC−C_{60} and TABC−C_{60} where TAiBC = tetraazaisobacteriochlorin and TABC = tetraazabacteriochlorin) have been synthesized by condensing 1,2-dicyanofullerene (**1**) and phthalonitrile derivatives (**2**) in the presence of nickel chloride in quinoline, and fully characterized using mass spectrometry and ^{1}H and ^{13}C NMR. By arranging the TAC and C_{60} units at the minimum distance, and taking also into account the molecular symmetry, the resultant conjugates show on−off electronic communication behavior, depending on the push−pull properties of the peripheral substituents in the TAC moiety. Consequently, the UV−vis absorption spectrum of the electron-releasing butyloxy-substituted TAC−C_{60} (**3a**) contains an unusual group of three absorption bands in the Q-band region (500−900 nm) as a result of a strong electronic communication between the two moieties. On the other hand, the absorption spectrum of the electron-withdrawing butylsulfonyl-substituted TAC−C_{60} (**3b**) comprises a typically normal TAC spectrum with markedly split two-peak Q-bands. A similar phenomenon is observed between alkoxy-substituted TAiBC−C_{60} (**4a**) and butylsulfonyl-substituted TAiBC−C_{60} (**4b**). This study reveals that the electron-donating or -withdrawing nature of the peripheral substituents on an azachlorin moiety has an important effect on the electronic structures of our novel azachlorin−C_{60} conjugates, although the linking carbon atoms are aliphatic sp^3 carbon atoms which generally do not contribute to aromaticity. The electronic structures of the conjugates have been investigated in detail using spectroscopic and electrochemical techniques with the aid of DFT calculations.

Introduction

Phthalocyanines (Pc's) are a very versatile class of heteroaromatic compound, and are well-known as one of the most important classes of industrial dye and pigment materials.[1] Recent advances in synthetic methods and chromatographic separation techniques have made possible a wide range of new Pc derivatives with different skeletons and substituents. Consequently, a variety of functionalized Pc derivatives have now become available, and their spectroscopic and electrochemical properties have been studied extensively in order to develop these for a wide variety of applications such as organic conductors, chemical sensors, catalysts, and read−write optical discs.[1,2] Recent academic developments of Pc's and Pc analogues have also been reviewed in several papers and books.[1−4]

The first covalently bonded Pc−fullerene (C_{60}) complex was reported as a "green fullerene" in 1995, in which the importance of the electron deficiency and the ability to undergo multistage reductions of C_{60} was described.[5] We anticipate that the possibility of developing new devices such as organic transistors and photovoltaic cells will increase if Pc and C_{60} are combined properly, since Pc's themselves have rich electronic properties. The Torres group has synthesized some photochemically active Pc− and subPc−C_{60} adducts which can form stable charge-separation states with high quantum yields.[6] Although the previously reported Pc−C_{60} conjugates have been shown to have remarkable redox properties due to the presence of the C_{60} units, the molecular orbitals (MOs) appear to be independent of each other, since the UV−vis absorption bands of the Pc−C_{60} compounds are similar in shape to the sum of those of the original Pc's and C_{60}'s, indicating that the MOs of the Pc moiety are essentially unperturbed by the C_{60} unit. Since the LUMO

(1) Leznoff, C. C., Lever, A. B. P., Eds. *Phthalocyanines: Properties and Applications*; VCH: New York, 1989−1996; Vols. 1−4.
(2) (a) Shirai, H., Kobayashi, N., Eds. Shirai, H., Kobayashi, N., Eds. *Phthalocyanines: Chemistry and Functions*; IPC: Tokyo, 1997. (b) Kadish, K. M., Smith, K. M., Guilard, R., Eds. *The Porphyrin Handbook*; Academic Press, San Diego, 2003; Vols. 15−20.
(3) (a) de la Torre, G.; Vaquez, P.; Agullo-Lopez, F.; Torres, T. *Chem. Rev.* **2004**, *104*, 3723. (b) O'Flaherty, S. M.; Hold, S. V.; Cook, M. J.; Torres, T.; Chen, Y.; Hanack, M.; Blau, W. J. *Adv. Mater.* **2003**, *15*, 19. (c) Claessens, C. G.; Gonzalez-Rodriguez, D.; Torres, T. *Chem. Rev.* **2002**, *102*, 835. (d) de la Torre, G.; Claessens, C. G.; Torres, T. *Eur. J. Org. Chem.* **2000**, 2821.
(4) Kobayashi, N.; Fukuda, T. In *Functional Dyes*; Kim, S., Ed.; Elsevier: Oxford, 2006; Chapter 1.
(5) Linssen, T. G.; Dürr, K.; Hanack, M.; Hirsch, A. *J. Chem. Soc., Chem. Commun.* **1995**, 103.
(6) (a) Guldi, D. M.; Zilbermann, I.; Gouloumis, A.; Vázquez, P.; Torres, T. *J. Phys. Chem. B* **2004**, *108*, 18485. (b) Gouloumis, A.; Liu, S.-G.; Sastre, Á.; Vázquez, P.; Echegoyen, L.; Torres, T. *Chem. Eur. J.* **2000**, *6*, 3600.
(7) Mizuseki, H.; Igarashi, N.; Bilosludov, R. V.; Farajian, A. A.; Kawazoe, Y. *Synth. Met.* **2003**, *138*, 281.

10.1021/ja0678323 CCC: $37.00

energy level of Pc is fairly close to that of C_{60},[7] Pc−C_{60} conjugates appear to be promising candidates for realizing strongly interacting π-electron systems, if the Pc and C_{60} moieties are disposed in close proximity and have the correct MO symmetry. This type of compound may also be useful for developing novel ambipolar organic field-effect transistors (OFETs) since Pc and C_{60} have been used as p-channel and n-channel semiconductors, respectively.[8] As important examples of highly interacting C_{60} conjugates, buckyferrocenes are known to show a substantial shift of charge density from the ferrocene unit to the C_{60} moiety,[9] while Kräutler previously reported porphyrin congeners by taking advantage of easily accessible zinc−tetrasulfoleno−porphyrinate as a reactive building block.[10]

Tetraazachlorins (TACs), tetraazaisobacteriochlorins (TAiBCs), and tetraazabacteriochlorins (TABCs) are chemically partially ring-reduced Pc analogues.[11,12] These are characterized by one (TAC) or two adjacently (TAiBC) or oppositely (TABC) reduced pyrrole ring moieties. Although the isolation of ring-reduced Pc's can be difficult due to their instability (a high tendency toward dehydrogenation of pyrrole β-hydrogen), we have recently succeeded in isolating stable TACs, TAiBCs, and TABCs using tetramethylsuccinonitrile, **6**, as hydrogenated sites.[13,14] In a continuation of this study, the structural characteristics of azachlorins are considered to be useful in order to synthesize reduced Pc−C_{60} diads or triads exhibiting electronic communication. Since 1,2-dicyanofullerene, **1**,[15] has a local structure (bold-lined region in Scheme 1) identical to that of **6**, **1** can be used as a starting material for the synthesis of azachlorin−C_{60} derivatives.

In this paper, we report the synthesis and electronic structures of novel Pc (or azachlorin)−C_{60} conjugates, which are obtained by the mixed condensation of **1** with phthalonitrile derivatives **2**. The electronic structures of these were investigated on the basis of UV−vis absorption, magnetic circular dichroism (MCD), electrochemical, and quantum chemical methods. Although the linking carbon atoms are aliphatic sp^3 carbons that generally do not participate in the aromatic structure, we show here that the MOs of azachlorins and C_{60} moieties do interact if the two moieties are arranged in the closest proximity with proper symmetry, depending on the electron density in the azachlorin skeletons, i.e., by changing the azachlorin peripheral substituents. TD-DFT calculations reveal that the LUMOs of C_{60} and azachlorin moieties have similar energies, and as a consequence, some of the key frontier π-MOs of the conjugates can be expressed as a linear combination of those of the two moieties.

Experimental Section

Synthesis. 1,2-Dicyanofullerene (**1**),[15] 4,5-dibutyloxyphthalonitrile (**2a**),[16] and 4,5-bis(butylsulfonyl)phthalonitrile (**2b**)[17] were prepared according to the methods described in the literature. Quinoline was distilled over CaH_2 under vacuum prior to use. The other reagents were used as supplied.

Preparation of 3a and 4a. A mixture of **1** (100 mg, 0.13 mmol), **2a** (70 mg, 0.26 mmol), nickel chloride dihydrate (22 mg, 0.13 mmol), and a catalytic amount of ammonium molybdate was suspended in distilled quinoline (1 mL) and heated at 190 °C for 2 h under argon. After cooling to room temperature, the reaction mixture was poured into methanol and the resultant precipitate filtered off. The filtrate was vacuum-dried and the residue separated using column chromatography (silica, $CHCl_3$). Dark-green portions with $R_f = 0.78$ (**3a**) and $R_f = 0.89$ (**4a**) were collected. These fractions were further purified using successive size exclusion chromatography (Bio-Beads S-x1, $CHCl_3$). Recrystallization from $CHCl_3$/methanol gave **3a** and **4a** in 5.4% (23 mg) and 1.0% (5.4 mg) yield, respectively. MASS (MALDI) (*m*/*z*): 1648 ($M^+ + 1$ for **3a**), 2148 (M^+ for **4a**). Anal. Found: C, 80.13; H, 3.89; N, 6.66 (**3a**). Calcd for $C_{110}H_{60}N_8O_6Ni$: C, 80.15; H, 3.67; N, 6.80; Anal. Found: C, 86.75; H, 2.46; N, 4.72 (**4a**). Calcd for $C_{156}H_{40}N_8O_4Ni$: C, 87.20; H, 1.88; N, 5.21. ^{1}H NMR (CS_2/$CDCl_3$ = 4:1, 500 MHz): for **3a**, δ = 1.04 (t, 6H, CH_3), 1.12 (t, 6H, CH_3), 1.13 (t, 6H, CH_3), 1.60−1.74 (m, 12H, CH_2), 1.90−2.06 (m, 12H, CH_2), 4.42 (t, 4H, OCH_2), 4.31 (t, 4H, OCH_2), 4.42 (t, 4H, OCH_2), 8.10 (s, 2H, aromatic), 8.14 (s, 2H, aromatic) 8.35 (s, 2H, aromatic); for **4a**, δ = 1.05 (t, 6H, CH_3), 1.15 (t, 6H, CH_3), 1.62 (sext, 4H, CH_2), 1.73 (sext, 4H, CH_2), 1.93 (quint, 4H, CH_2), 2.06 (quint, 4H, CH_2), 4.25 (t, 4H, OCH_2), 4.45 (t, 4H, OCH_2), 8.04 (s, 2H, aromatic), 8.35 (s, 2H, aromatic). ^{13}C NMR (CS_2/$CDCl_3$ = 4:1, 125 MHz): for **3a**, δ = 14.09, 14.16, 14.20, 19.66, 19.74, 19.76, 31.46, 31.68, 103.37, 104.22, 104.59, 128.63, 129.56, 130.70, 136.55, 140.90, 141.77, 141.91, 142.18, 142.55, 142.78, 144.02, 144.97, 145.07, 145.52, 145.74, 145.99, 147.07, 147.52, 148.06, 148.47, 151.05, 151.15, 152.14, 155.63, 192.38, 192.53; for **4a**, δ = 14.11, 14.12, 19.70, 19.77, 31.50, 31.63, 68.87, 102.95, 103.58, 127.14, 130.06, 136.19, 136.80, 140.73, 140.88, 141.30, 141.49, 141.72, 142.00, 142.08, 142.37, 142.50, 142.71, 143.88, 143.94, 144.81, 144.91, 145.12, 145.21, 145.30, 145.64, 145.68, 145.77, 145.80, 146.88, 146.99, 147.19, 147.57, 150.75, 152.02, 192.38, 192.57.

Preparation of 3b, 4b, and 5b. A mixture of **1** (100 mg, 0.13 mmol), **2b** (95 mg, 0.26 mmol), nickel chloride dihydrate (23 mg, 0.14 mmol), and a catalytic amount of ammonium molybdate was suspended in distilled quinoline (1 mL) and heated at 190 °C for 2 h under argon. After cooling to room temperature, the reaction mixture was poured into methanol and the resultant precipitate filtered off. The filtrate was vacuum-dried and the residue separated successfully using normal (silica, $CHCl_3$) and medium-pressure column chromatography (silica, toluene). Dark-green, reddish violet, and blue portions with $R_f = 0.13$ (**3b**), 0.50 (**5b**), and 0.16 (**4b**) with respect to $CHCl_3$ were collected. These fractions were further purified using successive size exclusion chromatography (Bio-Beads S-x1, $CHCl_3$). Recrystallization from $CHCl_3$/methanol gave **3b**, **4b**, and **5b** in 3.1% (16 mg), 0.3% (2.1 mg), and 0.7% (4.3 mg) yield, respectively. MASS (MALDI) (*m*/*z*): 1936 (M^+ for **3b**), 2342 ($M^+ + 1$ for **4b**), 2342 ($M^+ + 1$ for **5b**). Anal. Found: C, 67.82; H, 4.03; N, 5.19 (**3b**). Calcd for $C_{110}H_{60}N_8S_6O_{12}Ni$: C, 68.21; H, 3.12; N, 5.79; Anal. Found: C, 78.19; H, 2.55; N, 3.94 (**4b**), C, 79.52; H, 2.49; N, 4.01 (**5b**). Calcd for $C_{156}H_{40}N_8S_4O_8Ni$: C, 80.04; H, 1.72; N, 4.79. Calcd for $C_{156}H_{40}N_8S_4O_8Ni{\cdot}2H_2O$: C, 78.82; H, 1.87; N, 4.71. ^{1}H NMR (CS_2/$CDCl_3$ = 4:1, 500 MHz): for **3b**, δ = 0.9−0.13 (m, 18H, CH_3), 1.48−1.57 (m, 12H, CH_2), 1.85−1.97 (m, 12H, CH_2), 3.80 (t, 4H, OCH_3), 3.86 (t, 4H, OCH_3), 3.95 (t, 4H, OCH_3),

(8) (a) Dimitrakopoulos, C. D.; Malenfant, P. R. L. *Adv. Mater.* **2002**, *14*, 99. (b) Dodabalapur, A.; Katz, H. E.; Torsi, L.; Haddon, R. C. *Science* **1995**, *269*, 1560.
(9) Guldi, D. M.; Rahman, G. M. A.; Marczak, R.; Matsuo, Y.; Yamanaka, M.; Nakamura, E. *J. Am. Chem. Soc.* **2006**, *128*, 9420.
(10) Rieder, A.; Kräutler, B. *J. Am. Chem. Soc.* **2000**, *122*, 9050.
(11) Ficken, G. E.; Linstead, R. P.; Stephen, E.; Whalley, M. *J. Chem. Soc.* **1958**, 3879.
(12) (a) Makarova, E. A.; Korolyova, G. V.; Tok, O. L.; Luk'yanets, E. A. *J. Porphyrins Phthalocyanines* **2000**, *4*, 525. (b) Miwa, H.; Makarova, E. A.; Ishii, K.; Luk'yanets, E. A.; Kobayashi, N. *Chem. Eur. J.* **2002**, *8*, 1082.
(13) Makarova, E. A.; Fukuda, T.; Luk'yanets, E. A.; Kobayashi, N. *Chem. Eur. J.* **2005**, *11*, 1235.
(14) Fukuda, T.; Makarova, E. A.; Luk'yanets, E. A.; Kobayashi, N. *Chem. Eur. J.* **2004**, *10*, 117.
(15) Keshavarz, K. M.; Knight, B.; Srdanov, G.; Wudl, F. *J. Am. Chem. Soc.* **1995**, *117*, 11371.
(16) van der Pol, J. F.; Neeleman, E.; Zwikker, J. W.; Nolte, R. J. M.; Drenth, W. *Recl. Trav. Chim. Soc., Pays-Bas.* **1988**, *107*, 615.
(17) del Rey, B.; Keller, U.; Torres, T.; Rojo, G.; Agulló-López, F.; Nonell, S.; Martí, C.; Brasselet, S.; Ledoux, I.; Zyss, J. *J. Am. Chem. Soc.* **1998**, *120*, 12808.

Scheme 1. Synthesis of **3**−**5** and **7**[a]

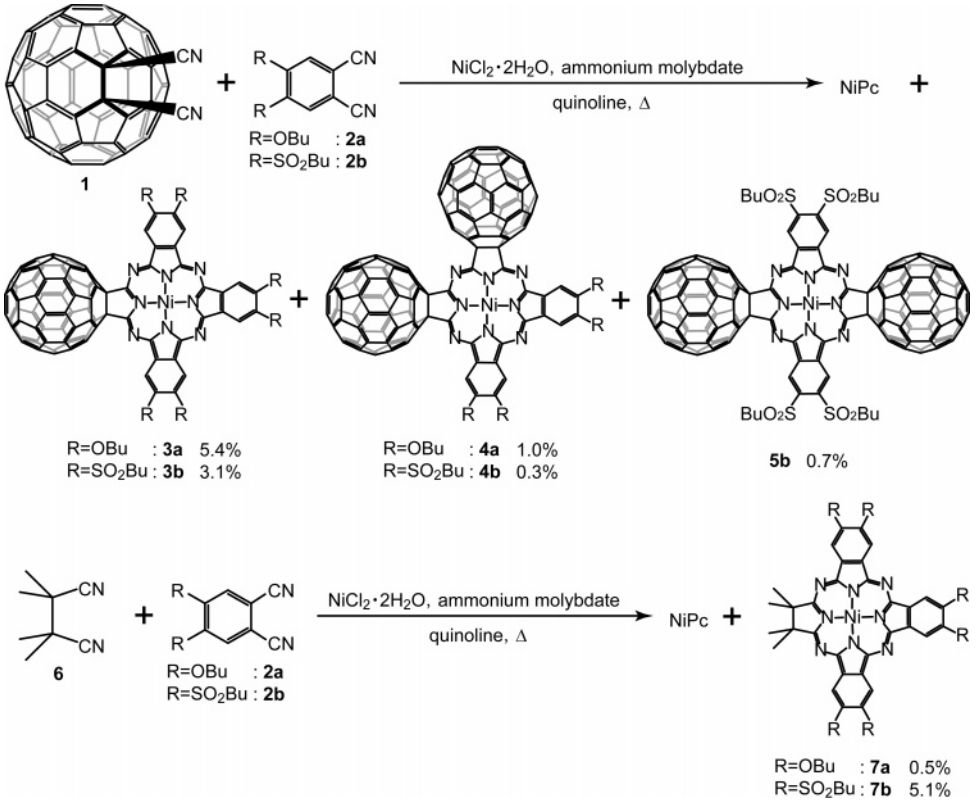

[a] Yields were calculated based on the amount of phthalonitrile used in the reaction.

9.80 (s, 2H, aromatic), 10.13 (s, 4H, aromatic), for **4b** ($CS_2/CDCl_3$ = 3:2, 600 MHz), δ = 0.82−2.44 (m, 28H, $CH_2CH_2CH_3$), 5.29 (t, 8H, OCH_2), 9.76 (s, 4H, aromatic), for **5b** ($CS_2/CDCl_3$ = 3:2, 400 MHz), δ = 0.95 (t, 6H, CH_3), 0.99 (t, 6H, CH_3), 1.52 (sext, 8H, CH_2), 1.85 (quint, 4H, CH_2), 1.92 (quint, 4H, CH_2), 3.75 (t, 4H, SO_2CH_2), 3.81 (t, 4H, SO_2CH_2), 9.56 (s, 2H, aromatic), 9.87 (s, 2H, aromatic).

Preparation of 7a. A mixture of **6** (50 mg, 0.36 mmol), **2a** (200 mg, 0.73 mmol), nickel chloride dihydrate (66 mg, 0.40 mmol), and a catalytic amount of ammonium molybdate was suspended in distilled quinoline (1 mL) and heated at 190 °C for 2 h under argon. After cooling to room temperature, the reaction mixture was poured into methanol and the resultant precipitate filtered off. The filtrate was vacuum-dried and the residue purified using column chromatography (silica, $CHCl_3$), thin layer chromatography (silica, toluene), and size exclusion chromatography (Bio-Beads S-x1, $CHCl_3$), followed by recrystallization from $CHCl_3$/methanol, to give **7a** in 0.5% (3.7 mg) yield. MASS (ESI-TOF) (*m*/*z*): 1011 ($M^+ + 1$). Anal. Found: C, 66.15; H, 7.20; N, 10.96. Calcd for $C_{56}H_{72}N_8O_6Ni$: C, 66.47; H, 7.17; N, 11.07. ^{1}H NMR ($CDCl_3$, 400 MHz): δ = 1.05 (t, 6H, CH_3), 1.06 (t, 6H, CH_3), 1.12 (t, 6H, CH_3), 1.63 (sext, 4H, CH_2), 1.70 (sext, 4H, CH_2), 1.80 (s, 12H, CH_3), 2.00 (quint, 8H, CH_2), 2.05 (quint, 4H, CH_2), 4.41 (t, 18H, OCH_3), 8.32 (s, 2H, aromatic), 8.52 (s, 2H, aromatic), 8.56 (s, 2H, aromatic).

Preparation of 7b. A mixture of **6** (37 mg, 0.27 mmol), **2b** (200 mg, 0.54 mmol), nickel chloride dihydrate (47 mg, 0.28 mmol), and a catalytic amount of ammonium molybdate was suspended in distilled quinoline (1 mL), and heated at 190 °C for 2 h under argon. After cooling to room temperature, the reaction mixture was poured into methanol and the resultant precipitate filtered off. The filtrate was vacuum-dried and the residue purified using thin layer chromatography (silica, $CHCl_3$), and size exclusion chromatography (Bio-Beads S-x1, $CHCl_3$), followed by recrystallization from $CHCl_3$/methanol, to give **7b** in 5.1% (36 mg) yield. MASS (ESI-TOF) (*m*/*z*): 1301 ($M^+ + 1$). HRMASS(ESI-FTICR)(*m*/*z*): 1321.2827. Calcd for $[M + Na]^+$: 1321.2840. ^{1}H NMR ($CDCl_3$, 400 MHz): δ = 0.88 (t, 6H, CH_3), 0.96 (t, 6H, CH_3), 1.01 (t, 6H, CH_3), 1.52 (sext, 12H, CH_2), 1.88 (quint, 12H, CH_2), 3.80 (t, 4H, SO_2CH_2), 3.86 (t, 8H, SO_2CH_2), 9,80 (s, 2H, aromatic), 10.1 (s, 4H, aromatic).

Measurements. Electronic absorption spectra were measured with a Hitachi U-3410 spectrophotometer. Magnetic circular dichroism (MCD) spectra were recorded using a Jasco J-725 spectrodichrometer with a Jasco electromagnet that produces a magnetic field of up to 1.09 T. The magnitude of the MCD signal is expressed in terms of molar ellipticity per tesla, $[\theta]_M$/deg mol^{-1} dm^3 cm^{-1} T^{-1}.

Cyclic voltammetry data were collected under a dry nitrogen atmosphere with a Hokuto Denko HA-501 potentiostat connected to a Hokuto Denko HB-104 function generator and a Graphtec WX1200 XY recorder. *o*-Dichlorobenzene (*o*DCB) was used as the solvent, with 0.1 mol/L tetrabutylammonium perchlorate (TBAP) as the supporting electrolyte. Glassy carbon (area = 0.07 cm^2) and Pt and Ag/AgCl wires were used as working, counter, and reference electrodes, respectively. The ferrocenium/ferrocene (Fc^+/Fc) couple was used as an internal standard.

Results and Discussion

Synthesis and Characterization. In our previous paper, we reported that the template reaction using nickel or vanadium chloride in the presence of ammonium molybdate is suitable for the synthesis of azachlorin derivatives.[13,14] In particular, nickel complexes are preferable in terms of yield and ease of characterization because diamagnetic nickel Pc's can be characterized by NMR, unlike paramagnetic vanadyloxy complexes. Although metal-free and/or zinc derivatives are attractive from the photochemical point of view, these are found to be difficult to synthesize because of their low stability (Zn complexes) and low yield (metal-free complexes). Therefore, we first attempted to prepare nickel complexes. In order to increase the solubility of the complex, butyloxy (OBu) or butylsulfonyl (SO_2Bu)

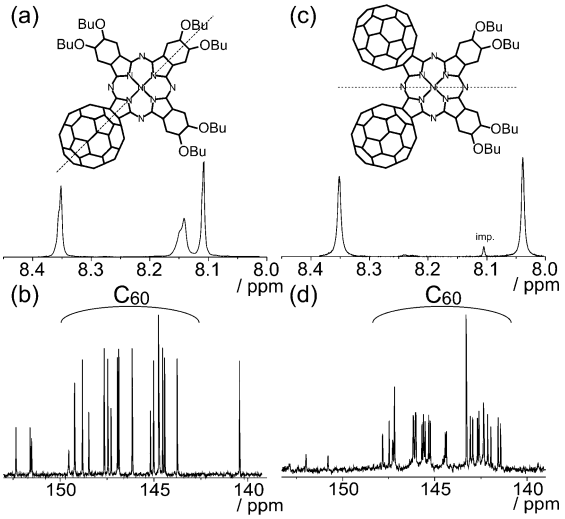

Figure 1. ^{1}H (top) and ^{13}C (bottom) NMR spectra of **3a** (left) and **4a** (right) in $CS_2/CDCl_3 = 4:1$ (v/v), respectively. The C_{60} carbon signals are specified in the figure.

groups were introduced at the peripheral positions of the Pc skeleton. It is well-known that alkylsulfonyl groups have strong electron-withdrawing properties, while alkyloxy groups show a moderate electron-donating nature. Mixed condensation of **1** and either **2a** or **2b** with a 1:2 molar ratio in the presence of nickel chloride and a catalytic amount of ammonium molybdate in quinoline at 190 °C, followed by purification by repeated silica gel and gel permeation (Bio-Beads S-x1) column chromatography, yielded **3a** and **4a** and **3b**, **4b**, and **5b**, respectively (Scheme 1). The OBu-substituted TABC−C_{60} conjugate was not obtained. Only **3a** or **3b** was obtained in the absence of ammonium molybdate. As a reference, C_{60}-free TACs (**7a** and **7b**) were synthesized similarly from **6** instead of **1** and either **2a** or **2b**. All complexes were characterized by mass and NMR. Figure 1 shows ^{1}H and ^{13}C NMR spectra of **3a** (left) and **4a** (right) in $CS_2/CDCl_3$ (4:1 v/v). The NMR data of the other compounds are supplied in the Supporting Information. The three types of aromatic proton appeared as singlet signals (8.10, 8.14, and 8.35 ppm) for **3a**, which is consistent with the structure expected from the mass. The 16 independent carbon signals appeared in the 142−150 ppm region, also lending support for the C_{2v} symmetry of **3a**. In the cases of TAiBC and TABC, we need to determine whether the molecules have a *cis* or *trans* structure. As shown in Figure 1c, two singlet aromatic protons were observed at 8.04 and 8.35 ppm, indicating that **4a** has a *cis*-type structure because only one aromatic signal is expected if the molecule was a D_{2h} *trans* isomer. In addition, the finely subdivided carbon signals (Figure 1d) also support the conclusion that the structure of this compound corresponds to **4a**.

Electronic Absorption and MCD Spectroscopy. Figure 2 shows the absorption and MCD spectra of **3** and **7** in $CHCl_3$. The Q spectral envelopes of **3a** and **7a** are quite different. Although both compounds exhibit medium intensity bands at 590−620 nm, the band at 734 nm in **7a** appears to split into two less-intense bands (699 and 773 nm) in **3a**, indicating strong interactions between the TAC and C_{60}. The MCD signs are positive for the former band and negative for the latter two. MCD theory suggests that oppositely signed Faraday *B* terms are expected if a transition couples with one that is orthogonal to it.[18] In this case, therefore, the two less-intense bands are

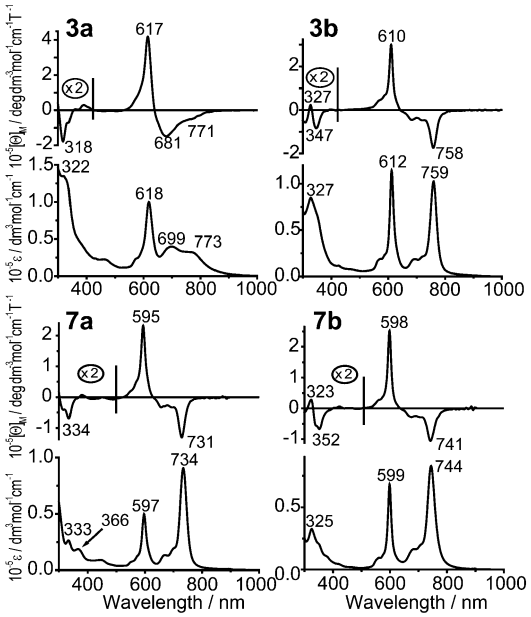

Figure 2. Absorption (bottom) and MCD (top) spectra of **3a** (top left), **3b** (top right), **7a** (bottom left), and **7b** (bottom right) in $CHCl_3$.

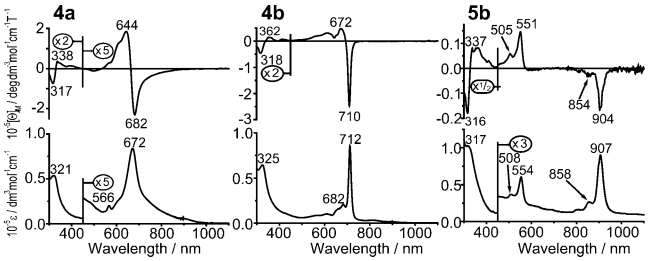

Figure 3. Absorption (bottom) and MCD (top) spectra of **4a** (left), **4b** (middle), and **5b** (right) in $CHCl_3$.

orthogonal to the other medium-intensity band, while the bands at 699 and 773 nm are not orthogonal to each other. In the case of the SO_2Bu-substituted species, the absorption spectrum of **3b** resembles that of the corresponding typical TAC (**7b**). Two intense absorption bands at 759 and 612 nm can be assigned as split Q bands, and the corresponding negative and positive MCD signals at 758 and 610 nm, respectively, lend strong support to this assignment (Figure 2, top right). When the bands of **3a** and **3b** are compared, those at shorter wavelength (ca. 610−620 nm) are similar in shape to each other, while the longer-wavelength components are completely different. Interestingly, **3a** and **3b** have the same aromatic skeleton, so that this difference should be attributed only to their peripheral substituents. The electronic structures of **3a** and **3b**, therefore, appear to be quite different.

The absorption spectra of the TAiBC derivatives (**4a** and **4b**) also show significant dependence on their peripheral substituents (Figure 3). Our previous study revealed that C_{60}-free TAiBC derivatives give very sharp Q absorption bands.[13,14] However, in the case of OBu-substituted **4a**, a broad, less-intense tail stretches beyond the Q-band into the near-IR region (ca. 680−1000 nm). It is difficult to estimate how many components are present in this tail. On the other hand, the intense Q-band component at 712 nm, as well as the corresponding large

(18) Rodger, A.; Nordén, B. *Circular Dichroism and Linear Dichroism*; Oxford University Press: Oxford, 1997.

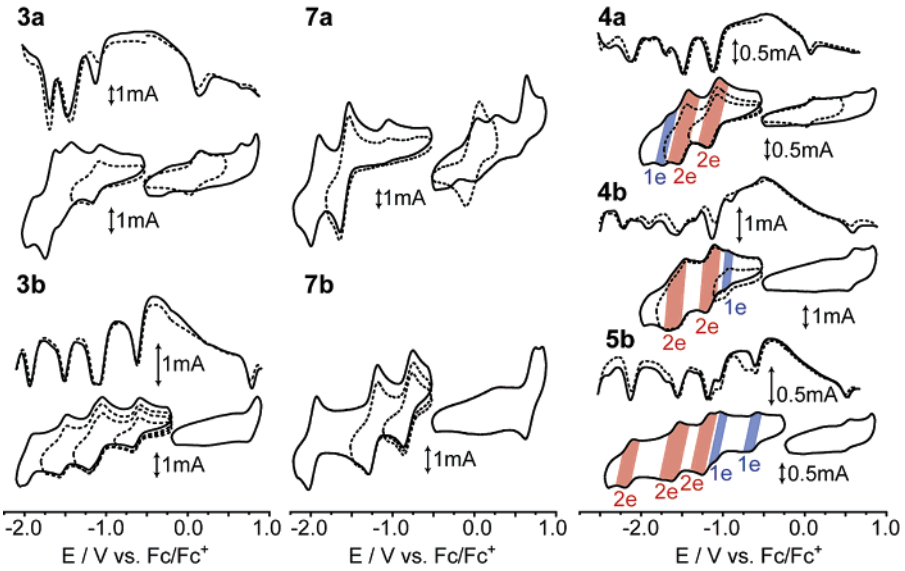

Figure 4. Cyclic voltammograms in *o*DCB containing 0.1 M TBAP. Sweep rate = 50 mV/s. Differential pulse voltammograms, recorded with a sweep rate of 5 mV/s, are also shown; solid lines indicate cathodic scanning and dashed lines, anodic scanning. The number of electrons involved in the redox processes is shown for the reduction side of **4a**, **4b**, and **5b**. The other couples are all one-electron processes.

Table 1. Redox Potentials/V vs Fc^+/Fc in *o*DCB Containing 0.1 M TBAP

compd	6th red.	5th red.	4th red.	3rd red.	2nd red.	1st red.	1st ox.
3a				−1.69	−1.45	−1.11	0.13
3b		−1.93	−1.51	−1.14	−1.08	−0.62	0.78
4a	−2.38	−2.10	−1.99	−1.64	−1.47	−1.11	0.07
4b	−2.24	−1.93	−1.57	−1.38	−1.14	−0.93	0.58
5b	−2.12	−1.69	−1.55	−1.18	−1.04	−0.61	0.52
7a					−1.59	−1.95	−0.02
7b				−1.96	−1.21	−0.79	0.70
C_{60}			−2.36	−1.90	−1.46	−1.07	

negative MCD signal of **4b**, indicates that the electronic structure of this compound is similar to that of the typical C_{60}-free TAiBC. The MCD spectra indicate that the band at 672 nm (**4a**) consists of two components, while that at 712 nm (**4b**) consists of one component, since the corresponding MCD signals are dispersion-type *A* term and Gaussian-type *B* term, respectively. The *trans* isomer (**5b**) shows two Q-band components at 554 and 907 nm, similarly to C_{60}-free TABC.[11,12] Since no OBu-substituted **5a** has been obtained, the effect of the peripheral substituents is unclear for the two C_{60}-containing *trans* isomers at present.

Electrochemistry. Figure 4 displays electrochemical data of the complexes in *o*DCB containing 0.1 mol dm^{-3} TBAP as the supporting electrolyte, with redox potential data tabulated in Table 1. The redox potentials were determined mostly on the basis of the cyclic voltammograms (CV). Differential pulse voltammograms (DPV) were also measured complementarily. It is well-known that the HOMO and LUMO energies of Pc or azaporphyrin derivatives correlate well with the first oxidation and reduction potentials.[14,19] Since Ni^{II} does not undergo redox processes within this potential window in *o*DCB,[20] the observed processes must be either Pc-ring- or C_{60}-centered. In addition, all oxidation processes can be ascribed as Pc-ring-centered because the HOMO of C_{60} is energetically low-lying and, therefore, not readily oxidized.[21] The first oxidation potentials shift to the positive by more than 500 mV and up to 720 mV when the SO_2Bu-substituted derivatives (**3b**, **4b**, and **7b**) are compared with the corresponding OBu-substituted derivatives (**3a**, **4a**, and **7a**, respectively), suggesting that the MO energies depend on the relative electron donating/withdrawing properties of the substituents. In a similar manner, comparison of **3a** and **7a** (or **3b** and **7b**) reveals that the introduced C_{60} units shift the first oxidation potentials positively. These observations indicate an electron-deficient nature of the SO_2Bu- and C_{60}-substituted Pc's. A similar trend is observed for the reduction potentials, although much more abundant reduction behavior is recorded for the C_{60}-fused derivatives.

Since **4a**, **4b**, and **5b** have two C_{60} moieties in the skeleton, simultaneous multi-electron reductions are expected. The CV of **4a** gives rise to one oxidation process at 0.07 V and three well-resolved reduction steps on the reduction side. Importantly, the peak currents (I_p) for the first two reduction processes are approximately twice as intense as those seen in the oxidation and third reduction, indicating that two electrons are involved in these processes. According to the Nernst equation, the peak potential difference, $\Delta E_p = E_{pc} - E_{pa}$, is given by $\Delta E_p = 59/n$ mV, where n is the number of electrons involved, which means that a smaller ΔE_p is expected for multi-electron steps. However, the ΔE_p for the first two reduction processes of **4a** is substantially larger than that of the oxidation process. Therefore, we conclude that two one-electron reduction processes occur simultaneously or at very close potentials rather than a so-called a two-electron process. Probably, the existence of two C_{60} units is essential for this observation, where each C_{60} unit appears to receive one electron almost simultaneously. It is, therefore, conceivable that the first and second reductions of **4a** are C_{60}-centered and that the third is Pc-centered. In addition, comparison of **4a** with the C_{60}-free reference compound[14] also supports these assignments, since the observation that the first reduction couple of nickel TAiBC lies at −1.79 V implies that

(19) (a) Fukuda, T.; Homma, S.; Kobayashi, N. *Chem. Eur. J.* **2005**, *11*, 5205. (b) Kobayashi, N.; Fukuda, T. *J. Am. Chem. Soc.* **2002**, *124*, 8021. (c) Kobayashi, N.; Miwa, H.; Nemykin, V. *J. Am. Chem. Soc.* **2002**, *124*, 8007.
(20) Lever, A. B. P.; Milaeva, E. R.; Speier, G. in ref 1, Vol. 3, Chapter 1.
(21) (a) Hirsch, A.; Brettreich, M. *Fullerenes*; Wiley-VCH: Weinheim, 2005. (b) Kadish, K. M., Ruoff, R. S., Eds. *Fullerenes: Chemistry, Physics, and Technology*; Wiley-Interscience: New York, 2000.

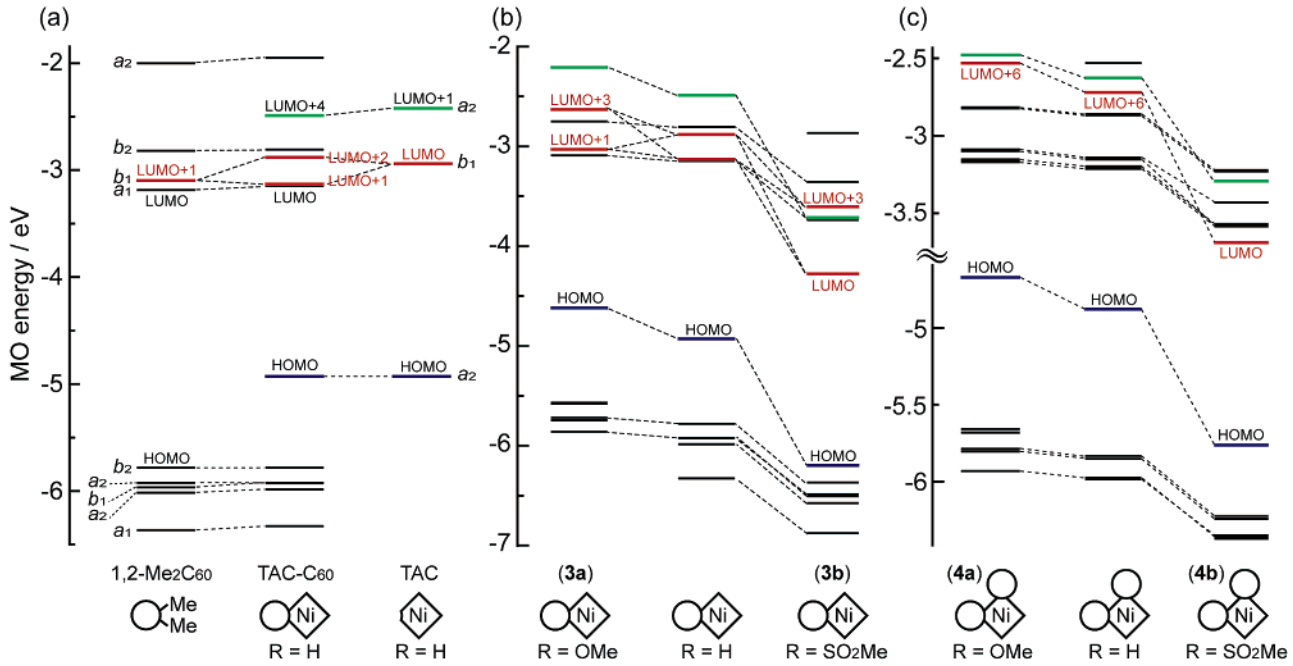

Figure 5. Partial MO energy diagram of (a) 1,2-$C_{60}(Me_2)$ (left), unsubstituted TAC−C_{60} (middle), and C_{60}-free TAC (right); (b) **3a*** (left), unsubstituted TAC−C_{60} (middle), and **3b*** (right); and (c) **4a*** (left), unsubstituted TAiBC−C_{60} (middle), and **4b*** (right). Note that the MO energy of 1,2-$C_{60}(Me_2)$ and TAC is corrected so that the HOMO of 1,2-$C_{60}(Me_2)$ and HOMO−1 of TAC−C_{60}, and the HOMO of TAC and HOMO of TAC−C_{60}, respectively, have identical energies.

the first two reduction couples of **4a** at −1.11 and −1.45 V are C_{60}-centered. Similarly, the second and third reductions of **4b** can be ascribed to two almost-simultaneous one-electron processes. To summarize, the electrochemical data indicate that the first reduction of **4b** occurs on Pc (or azachlorin), whereas that of **4a** is C_{60}-centered. In the case of **5b**, five redox couples were recorded on the reduction side. From the CV, the first two appear to be one-electron processes, while the other three may involve two electrons.

Electronic Structures. In order to understand the electronic structures of the complexes, the molecular orbitals (MOs) and the excitation energies were calculated. The molecular geometries were first optimized at the DFT level using the B3LYP/3-21G combination of the hybrid functional and basis set, as implemented in Guassian03, followed by DFT and TDDFT calculations within the B3LYP/6-31G(d) level. Only DFT calculations were performed for TAiBC−$(C_{60})_2$ since the molecular size is beyond the capacity of our computing resources for TDDFT calculations. To simplify the calculations, the complexes are assumed to have C_{2v} symmetry and the OBu and SO_2Bu groups are replaced with OMe and SO_2Me groups, respectively (we denote **3a***, **3b***, and so forth). The unsubstituted derivatives, where R = H, were also calculated. Partial MO energy diagrams of 1,2-dimethyl C_{60} (1,2-Me_2C_{60}), unsubstituted TAC−C_{60}, and unsubstituted TAC are shown in Figure 5a in order to clarify how the C_{60} and TAC moieties interact. Figures 5a and 6a demonstrate that the MO energies and distribution of the MO coefficients of TAC−C_{60} strongly reflect those of the TAC and C_{60} components. For example, the HOMO and LUMO of TAC−C_{60} originate from the HOMO of TAC and LUMO of 1,2-Me_2C_{60}, respectively, i.e., the MO coefficients of the HOMO and LUMO of TAC−C_{60} are almost identical to the HOMO of TAC and the LUMO of 1,2-Me_2C_{60}, respectively. This type of localized MOs is predicted for most of the MOs of TAC−C_{60}. The HOMO−1 to HOMO−4 are dominated by the low-lying C_{60} orbitals. The calculations also predict that some of the MOs are delocalized over the entire complex. The LUMO+1 and LUMO+2 are of this type, and can be expressed as a linear combination of the LUMO+1 of 1,2-Me_2C_{60} and LUMO of TAC. This kind of interaction is only observed when the two components are in close enough proximity for the π-orbitals to overlap and have the same symmetry.[22] In other words, the initial LUMO of TAC splits into two delocalized orbitals in the presence of the C_{60} unit. As a consequence, the three absorption bands (i.e., bands at 618, 699, and 773 nm in **3a**, Figure 2) can be assigned as transitions mainly from the HOMO to LUMO+1, LUMO+2, and LUMO+4, respectively. Since the LUMO+4 is almost identical to the LUMO+1 of the constituted TAC, the HOMO→LUMO+1 transition of TAC is changed to the HOMO→LUMO+4 transition of TAC−C_{60}. Figure 6a indicates that the LUMO+1 and LUMO+2 of TAC−C_{60} are predicted to be parallel to each other and are both orthogonal to the LUMO+4. This assignment is consistent with the observed experimental MCD behavior. The HOMO→LUMO and HOMO→LUMO+3 transitions are energetically comparable to the observed Q bands, although these are practically forbidden due to the small MO overlaps between the initial and final MOs.

We further compare the effects of substituents by calculating OMe- or SO_2Me-substituted TAC−C_{60} and TAiBC−$(C_{60})_2$ (Figure 5b,c). Unexpectedly, the calculations for the unsubstituted TAC−C_{60} explain the experimental spectrum of **3a** better than the calculated results for OMe-substituted derivative **3a***, while the spectrum of **3b** is reasonably reproduced by the SO_2-Me-included calculations. The MO mixings are sensitive to the relative MO energies of the constituent moieties (TAC and C_{60}). Although alkyloxy groups act as moderate electron donors, the

(22) The resonance integral, h_{ab}, is expected as $h_{ab} \approx {}^1/_2 S_{ab}(h_{aa} + h_{bb})$ by the Mulliken approximation, where S_{ab}, h_{aa} (h_{bb}) are the overlap and Coulombic integrals, respectively.

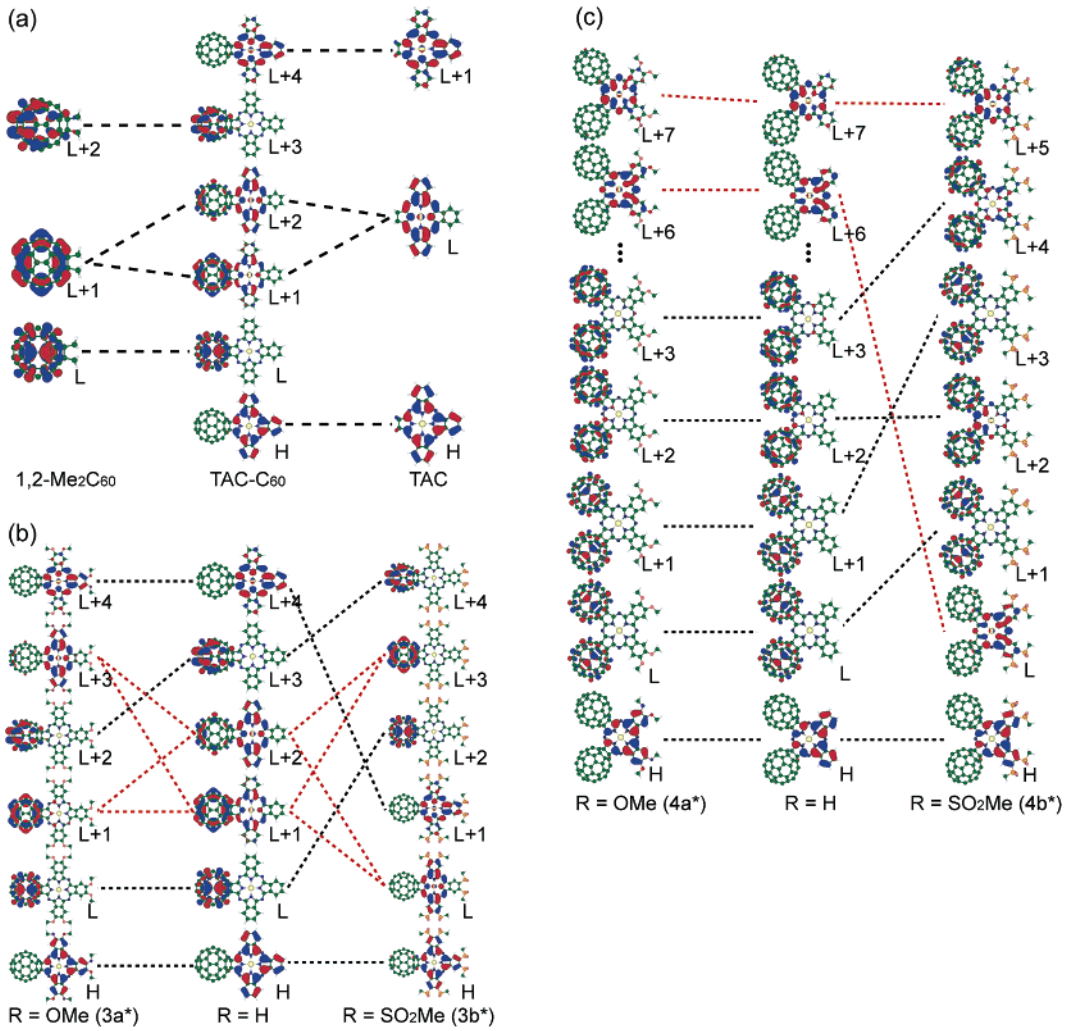

Figure 6. MOs which are principally associated with the Q bands. The HOMO and LUMO are represented as H and L, respectively.

DFT calculations cannot sufficiently reproduce the absolute MO energies for the OMe- and un-substituted derivatives, since there is only a slight difference between these. Therefore, we use the calculated results for the unsubstituted derivatives to understand **3a**. On the other hand, the spectral characteristics of **3b** are well reproduced by the calculations, since the SO_2Me group functions as a very strong electron acceptor which greatly stabilizes the MO energies. Figure 5b reveals that the DFT calculations reflect fairly well the substituent effects, where the corresponding MOs are stabilized in the order −OMe, −H, and $-SO_2Me$. In particular, the stabilization is significant for the TAC-centered MOs, since the TAC skeletons are directly affected by the substituents. Although the occupied orbitals show parallel shifts, some of the unoccupied orbitals change their order between the −H and $-SO_2Me$ derivatives. As a consequence, the MO mixing seen in the LUMO+1 and LUMO+2 of the −H derivative is removed, to generate C_{60}-centered LUMO+3 and TAC-centered LUMO. Similarly, the LUMO+4 of the −H derivative is stabilized to the LUMO+1 in the $-SO_2Me$ derivative **3b***. Since two split Q-band components were observed in the absorption spectrum of **3b** (Figure 2), the calculated results are consistent with the observed spectrum, where the two observed Q bands can be assigned to the HOMO→LUMO (759 nm) and HOMO→LUMO+1 (612 nm) transitions. The C_{60} moiety of **3b** is hardly involved in the Q-band transitions.

In the case of the TAiBC−C_{60} systems (R = H, OMe), the LUMO+6 and LUMO+7 are the TAiBC-centered unoccupied orbitals (Figure 6c). Therefore, the band at 672 nm for **4a** is composed of the HOMO→LUMO+6 and HOMO→LUMO+7 transitions. This assignment is consistent with the observed dispersion-type MCD signals. Although the low-lying unoccupied orbitals are mainly C_{60}-centered, their MO coefficients spread to some extent over the TAiBC moiety. It is conceivable that the broad, less-intense tail on the longer-wavelength side (Figure 3, left) is composed of the HOMO→LUMO+2 and HOMO→LUMO+3 transitions. By changing the substituents to the SO_2Bu group, the LUMO+6 is markedly stabilized to the LUMO (Figure 6c). As a result, the Q-band at 712 nm for **4b** (Figure 3, center) is now assigned as the HOMO→LUMO transition. The calculations indicate that the LUMO and LUMO+1 of **4a** (Figure 5, right) are almost degenerate and that these are localized on the two C_{60} moieties. Therefore, simultaneous two-electron reductions are expected for this compound. By changing the substituents to SO_2Bu groups, the LUMO+6 of **4a** is stabilized to the LUMO. As a result, a one-electron process is expected for the first reduction couple of **4b**, since the LUMO of **4b** is TAiBC-centered. As described in

the electrochemistry section, we indeed observed that the first reduction couples consist of a two-electron process for **4a** and a one-electron process for **4b**, supporting our assignments.

Conclusions

In summary, we have reported the use of 1,2-dicyanofullerene, **1**, enables the introduction of C_{60} units into TAC, TAiBC, and TABC ligands. Compound **1** and phthalonitrile derivatives **2** react to give novel C_{60}−TAC, C_{60}−TAiBC, and C_{60}−TABC conjugates in the presence of nickel chloride as a template, in which the chromophores and C_{60} are linked directly at the minimum distance. The absorption spectrum of alkoxy-substituted **3a** is clearly different from that of the corresponding C_{60}-free TAC (**7a**), suggesting a significant effect of the C_{60} unit on the electronic structure of the TAC moiety. DFT calculations indicate that **3a** exhibits extensive MO mixing between the C_{60} and TAC moieties, as a result of the close energies of the frontier orbitals, and the rigid and close arrangement taking the symmetry into account. Thus, some of the key frontier MOs of **3a** are based on a linear combination of the C_{60} and TAC moieties. On the contrary, **7b** and SO_2Bu-substituted **3b** show very similar absorption spectra, since the electron-withdrawing SO_2Bu groups lower the MO energies of the TAC moiety to remove the MO mixing. As a consequence, the MOs of **3b** are localized on each moiety, so that the delocalized LUMO+1 and LUMO+2 of **3a** are transformed into C_{60}-centered LUMO+3 and TAC-centered LUMO in the electron-withdrawing alkylsulfonyl-substituted **3b**. Similarly to the TAC derivatives, TAiBC−C_{60} conjugates also show significant substituent effects on their electronic structures. The electrochemical study has revealed that the LUMO of electron-releasing alkoxy-substituted **4a** is C_{60}-centered, while the LUMO of electron-withdrawing group-substituted **4b** is TAiBC-centered, which is consistent with the calculated electronic structures.

In this study, we have demonstrated that the presence of peripheral C_{60} units has a remarkable effect on the electronic structures of the phthalocyanine analogues (azachlorins). Interestingly, we have observed that the spectroscopic behavior is significantly affected by the peripheral substituents on the ligands, even when the aromatic skeletons are identical. This kind of drastic spectroscopic effect induced by the presence of the C_{60} moiety, as well as the characteristic structural features, has not been reported to date. To our knowledge, this is the first example showing clear MO mixing between the C_{60} and linked chromophores. This mixing is observed even when aliphatic sp^3 carbons are intercalated between two sp^2 carbons, as shown in our present case. This is because of the nonzero overlap integrals between the π-orbitals of planar Pc analogues and the spheric C_{60} moiety.

Acknowledgment. This research was supported by a Grant for Encouragement of Young Scientists (B) No. 17750029 and by a Grant-in-Aid (17350063) for Scientific Research and the COE project, Giant Molecules and Complex Systems, 2006 from the Ministry of Education, Culture, Sports, Science, and Technology, Japan. T.F. is grateful to Casio Science Promotion Foundation and Exploratory Research Program for Young Scientists from Tohoku University for their financial support. We also thank Prof. N. Ishikawa for valuable comments and discussion.

Supporting Information Available: Computational details; ^{1}H NMR of **3a**, **3b**, **4a**, **4b**, and **5b**; ^{13}C NMR of **3a**; MOs of unsubstituted TAC−C_{60}. This material is available free of charge via the Internet at http://pubs.acs.org.

JA0678323